GUMICS-3 — A GLOBAL IONOSPHERE-MAGNETOSPHERE COUPLING SIMULATION WITH HIGH IONOSPHERIC RESOLUTION

P. Janhunen

Finnish Meteorological Institute, Geophysical Research
P.O.B. 503, FIN-00101, Helsinki, Finland
phone: +358 9 19294635, fax: +358 9 19294603
email: Pekka.Janhunen@fmi.fi
Also at: Swedish Institute of Space Physics, Uppsala Division, 755 91, Uppsala, Sweden

Abstract

The prediction of satellite charging and other harmful effects can not be successful unless we can model and predict substorms and auroral breakups. For this we need a high-resolution global simulation system whose only essential input is the solar-wind data. GUMICS-3 ("Grand Unified Ionosphere-Magnetosphere Coupling Simulation, version 3") is a simulation system, which integrates a three-dimensional global magnetohydrodynamic (MHD) simulation box with a high-resolution model of ionospheric electrodynamics. We use a hierarchical cubic grid, which is recursively refined according to a specified grid point density function. The density function is such that the grid resolution is high in the near-Earth region, at the magnetopause and in the tail current sheet, while the solar wind, far tail and lobe regions have a lower resolution. The finite volume method (FVM) is used in the MHD equations [*Tanaka, 1994*]. The ionospheric conductivities depend on the electron precipitation, along with a dayside enhancement due to solar UV radiation. A model for the field-aligned potential drop (current-voltage relationship) also needs to be defined. The most important difference between GUMICS-3 and other similar programs is the use of a locally varying timestep. In the near-Earth region the Alfven speed is very high, which makes it necessary to use a very small timestep, sometimes less than 10 ms. In conventional simulation methods the same timestep must be used throughout the grid, but in our version of MHD the timestep is locally adaptive. This results in significant reduction (at least one order of magnitude) of computing time, making it possible to use a previously unavailable resolution in the near-Earth region and in the ionosphere without increasing the computer requirements. The grid spacing in the auroral ionospheric is less than 100 km in the supercomputer versions of the model.

1. Introduction

Satellite charging and other harmful effects caused by energetic particles in the Earth's plasma environment can be predicted in principle by two different types of methods. First, one can use detailed physics-based numerical simulation models, which is the subject of this paper. Second, one can use neural networks and other machine learning tools for the prediction of various indices describing the disturbance level (Kp, Dst, etc.) [*Lundstedt and Wintoft, 1994, Vassiliadis et al., 1995*]. In both cases the most important input is the solar wind. Ignoring spatial inhomogeneities, the solar wind input can be measured by a single satellite suitably positioned on the sunward side of the magnetosphere. The input quantities are the plasma density, temperature, velocity and magnetic field vector. How important the solar wind inhomogeneities are is not yet clear to us. One motivation of this research is to answer this question.

If the input time series is measured by a satellite, the time required to do the numerical computation is of the order of one hour (the time it takes for the solar wind to flow from the satellite to the dayside magnetopause). If longer time spans are needed, we must resort to other, indirect, methods to determine the solar wind data. We have not yet tried to use measured solar wind data with GUMICS-3, but have done so with an earlier version of the program [*Janhunen et al., 1996*]

Global magnetohydrodynamic (MHD) simulation of the Earth's magnetosphere has shown its effectiveness in giving accurate predictions for the overall geometry of the magnetosphere [e.g., *Ogino, 1986, Watanabe and Sato, 1990, Raeder et al., 1995, Fedder et al., 1995, Tanaka, 1995*]. Thus it is natural to base a magnetospheric simulation on the MHD equations, while keeping in mind that the validity of the MHD equations is mathematically speaking questionable in a collisionless plasma. However, MHD alone is not sufficient to make an ionosphere–magnetosphere coupling simulation because for the ionosphere, quite different kinds of equations apply (see below).

In order to model the ionosphere accurately (smallest grid spacing less than 100 km), the MHD resolution in the near-Earth region (3-5 R_E radial distance) must be high, about 0.1 R_E. There are two problems in the numerical realization of this. The

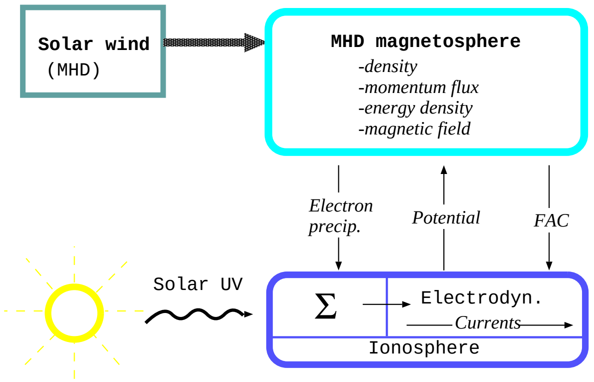

Figure 1: The overall structure of the GUMICS model

first problem is that we cannot hope to fill the whole magnetosphere, which is at least $150R_E$ in length, with $0.1R_E$ grid cells because that would yield several billion grid cells, which is not something we can afford now or in the near future. Thus the spatial MHD grid must be strongly nonuniform, with dense grid in the near-Earth region and sparse grid in the solar wind and in the far tail. The second problem, which is a more difficult one, is that in any explicit time differencing scheme, the timestep Δt must obey the Courant-Friedrichs-Lewy (CFL) condition: the timestep must be everywhere smaller than the fastest MHD wave travel time across the grid cell. In the near-Earth region the fastest wave phase speed is practically speaking equal to the local Alfvén speed $v_A = B/\sqrt{(\mu_0\rho)}$. Typically v_A in this region is about 20 000 km/s, which gives us a timestep of 0.02 seconds if $0.1R_E$ grid cells are used. Our approach to deal with this problem is to use a locally varying timestep [*Janhunen et al., 1996*].

2. Simulation model

The overall structure of the simulation is shown in **Figure 1**. We have a large simulation box which covers the whole magnetosphere, except the very far tail region. Magnetohydrodynamic (MHD) equations are used in the box. The initial condition is a magnetic dipole in homogeneous, cold and tenuous plasma, with a mirror dipole on the sunward side [*Raeder et al., 1995*] to make B_x zero on a particular YZ plane. The mirror dipole is required to create a "seed" magnetopause in the initial state. The existence of the mirror dipole does not affect the results at all once the simulation has properly started. At time $t = 0$ we turn on an incoming solar wind at $X = +32R_E$. X, Y, Z are the geocentric solar magnetospheric (GSM) coordinates, measured in Earth radii R_E, with the X axis towards the Sun and the Z axis northward along the dipole axis (more accurately: the projection of the dipole axis on a plane perpendicular to X). The Y axis completes the right-handed rectangular coordinate system and points towards eveningside. After about 40 minutes, the basic magnetospheric geometry becomes recognizable: the bow shock, the magnetopause, the magnetosheath, the cusp, the tail current sheet and the plasma sheet become identifiable. For this to happen, only the MHD equations are needed.

The ionosphere is a conducting plane, where the conductivity depends on solar ultraviolet (UV) radiation (dayside conductivity enhancement) and on magnetospheric particle precipitation (in this work only electron precipitation is taken into account). The magnetosphere affects the ionosphere in two ways: (1) by giving the electron precipitation which determines the ionospheric conductivity pattern, (2) by giving the field-aligned current (FAC) pattern. The field-aligned current is computed at the $3.7R_E$ shell, which is the inner boundary of the MHD equations. The region between the ionosphere and the $3.7R_E$ shell is assumed to be a passive medium which transmits the electric effects between the ionosphere and magnetosphere and where no magnetic field perpendicular currents flow (force-free region). The magnetic field inside $3.7R_E$ radius is assumed to be the dipole field. When the FAC and ionospheric conductivity (actually both Pedersen and Hall conductivity) are known, it is possible to solve the problem of horizontal current distribution in the ionosphere. This can be reduced to solving a 2D elliptic boundary value problem for the electric potential in the ionospheric plane [e.g., *Janhunen and Huuskonen, 1993*]. Once the ionospheric potential is known, we map it to the $3.7R_E$ shell, by also including a parallel electric field contribution (see below). Now that we know the magnetospheric electric potential at the inner edge of the MHD equations, we compute the corresponding $\mathbf{E}\times\mathbf{B}$ velocity, which is finally used as a boundary condition to the MHD equations. This is the only effect that the ionosphere has on the magnetosphere. The ionosphere/magnetosphere feedback loop is computed every four seconds, but the MHD time stepping is much more frequent.

In this work we write the MHD equations in fully conservative form and expand the magnetic field as $\mathbf{B} = \mathbf{B}_0 + \mathbf{B}_1$, where $\mathbf{B}_0$ is the background dipole field. Below we write the MHD equations without this complication, however, to save space. Otherwise our development follows closely the method of *Tanaka* [1994]: we use a linearized Riemann solution at every cell interface and the Godunov method [*LeVeque, 1992*]. (We have also programmed the MUSCL method which was used by Tanaka but the results reported in this paper use the Godunov method). We do not repeat here any of the details of the method, but only note the differences between our work and Tanaka's. Using fully conservative equations instead of the primitive variable formulation or a semiconservative formulation [*Raeder et al., 1995*] is theoretically more pleasing and enables us to get exact numerical conservation of mass, energy and momentum if wanted. The difficulty with the fully conservative method is that the pressure P must be computed by subtracting the kinetic and magnetic energy densities from the total energy density u. In low-beta plasma this subtraction is between two quantities which are numerically nearly equal, which amplifies any numerical inaccuracies and may even produce negative pressures. In practice one has to use use Tanaka's decomposition ($\mathbf{B} = \mathbf{B}_0 + \mathbf{B}_1$) to overcome this problem. Another possible problem with the fully conservative formulation is that spurious magnetic field parallel forces may appear. In the primitive variable formulation the Lorentz force is $\mathbf{j}\times\mathbf{B}$, which is also numerically exactly perpendicular to $\mathbf{B}$, but this is not the case in the fully conservative formulation.

The flux computation routine needs, among other things, the background magnetic field $\mathbf{B}_0$ at the cell interfaces. We found it necessary to compute surface integrals of $\mathbf{B}_0$ over the square shaped cell interfaces. The integrals can be computed analytically for a dipole field. Averaging $\mathbf{B}_0$ over each cell interface ensures that the numerical divergence of $\mathbf{B}_0$ on every cell is zero within roundoff error. Using pointwise values of $\mathbf{B}_0$ would introduce a spurious $\nabla\cdot\mathbf{B}_0$ of finite magnitude, which would cause serious convergence problems. This point was not explicitly mentioned in Tanaka's papers.

Our earlier program version GUMICS-2 [*Janhunen et al., 1996*], which also employed a locally varying timestep and hierarchical cubic grid as did *Gombosi et al.* [1996], used the primitive variable formulation and a classical, "high diffusion" spatial differencing scheme (the Lax method [*Press et al., 1992*]). The results were otherwise equal to the present results but contained more smeared profiles of the MHD variables because of higher numerical diffusion. Thus the present simulation (GUMICS-3) is a significant improvement over GUMICS-2.

We now define the model in equation form. The MHD equations are:

$$\frac{\partial \rho}{\partial t} = -\nabla\cdot(\rho\mathbf{v}), \tag{1}$$

$$\frac{\partial \mathbf{p}}{\partial t} = -\nabla\cdot\left(\frac{\mathbf{p}\mathbf{p}}{\rho} + P + \frac{B^2}{2\mu_0} - \frac{1}{\mu_0}\mathbf{B}\mathbf{B}\right) \tag{2}$$

$$\frac{\partial u}{\partial t} = -\nabla\cdot\left[(u + P - \frac{B^2}{2\mu_0})\frac{\mathbf{p}}{\rho} + \frac{1}{\mu_0}(\mathbf{B}\times\frac{\mathbf{p}}{\rho}\times\mathbf{B})\right], \tag{3}$$

$$\frac{\partial \mathbf{B}}{\partial t} = -\nabla\times\mathbf{E}, \qquad \nabla\cdot\mathbf{B} = 0, \tag{4}$$

$$\mathbf{E} + \mathbf{v}\times\mathbf{B} - \frac{1}{en}\mathbf{j}\times\mathbf{B} = 0, \qquad \mathbf{j} \equiv \frac{1}{\mu_o}\nabla\times\mathbf{B} \tag{5}$$

$$P \equiv (\gamma - 1)\left(u - \frac{\mathbf{p}^2}{2\rho} - \frac{\mathbf{B}^2}{2\mu_0}\right), \qquad \mathbf{p} \equiv \rho\mathbf{v} \tag{6}$$

The ionospheric model equations are similar to our earlier works [*Janhunen and Huuskonen, 1993, Janhunen et al., 1995, Janhunen et al., 1996*]. We have the height-integrated current continuity equation,

$$-\nabla\cdot\left(\Sigma_P\nabla\Phi_i + \Sigma_H\hat{\mathbf{b}}\times\nabla\Phi_i\right) = j_\parallel^{(i)}\sin I, \tag{7}$$

$$\Sigma_{P,H} = \int dh F_{P,H} n \tag{8}$$

where the coefficients $F_{P,H}$ tell how to obtain the local Pedersen (P) and Hall (H) conductivity values from the electron density n. The electron density n is solved in a 3D ionospheric grid using 20 nonuniform levels in height,

$$\frac{\partial n}{\partial t} = q - \alpha n^2 \tag{9}$$

where α is the coefficient of recombination and q is the ionization production rate caused by magnetospheric processes,

$$q = Q(\chi\rho, T, \Phi_m - \Phi_i), \tag{10}$$

where Q is a precomputed, tabulated function of three arguments: the source plasma density, temperature and the local magnetosphere-ionosphere parallel potential drop. For the definition of χ, see the discussion below. The parallel potential drop is assumed to be related to the field-aligned (parallel) current density by the formula

$$\Delta\Phi \equiv \Phi_m - \Phi_i = \begin{cases} \frac{j_\parallel^{(i)}}{K} - \frac{k_B T}{e} & , j_\parallel^{(i)} \le 0 \\ 0 & , \text{otherwise} \end{cases} \tag{11}$$

where positive current is downward. Here K is the Lyons-Evans-Lundin parameter, which in the present simulation is computed from

$$K = \frac{\chi n e^2}{\sqrt{2\pi m_e k_B T_e}} \tag{12}$$

according to *Fridman and Lemaire* [1980], equation 12. The factor χ is the loss cone filling rate, which is a dimensionless number between 0 and 1. Zero χ means that no new electrons arrive to the loss cone during one electron bounce period and unit χ means that the loss cone is completely filled with thermal electrons during one bounce period (strong pitch angle scattering). In case of zero χ, the field-aligned conductance K would be zero, and the ionization production q would vanish as well. Within MHD equations there is no self-consistent way to compute χ, so we are using an analytic model: Inside the polar cap χ is very close to unity and drops to a small value (0.02) at the equatorward edge of the mean auroral oval. Between these extremes (i.e., within the auroral oval) χ varies smoothly and monotonically. In addition, we include another contribution for χ, which is proportional to $\tau_B(1/T)\max(0, \mathbf{v}\cdot\nabla T)$. Here τ_B is an approximation to the electron bounce period and T is the local MHD plasma temperature. This expression tries to model the adiabatic heating of the particles in regions where plasma convects towards the Earth ($\mathbf{v}\cdot\nabla T > 0$). If χ thus computed becomes larger than one, it is set equal to one.

The locally varying time stepping scheme in the present model is similar to the one described by *Janhunen et al.* [1996]. The program has been written using the Tela programming language [*Janhunen, 1994-1996*], except that the MHD solver, which is the most time consuming part, has been written in `C++` and linked to Tela. The model is fully vectorized and is usually run on Cray C90 and achieves 200-300 MFLOPS (million floating point operations per second) performance. The results presented here use about 180 000 grid cells. With this spatial grid the model is usually 3-5 slower than real time (the variability of the performance figures is due to the adaptivity in time stepping). As mentioned above, our spatial grid is of the hierarchical cubic type [*Gombosi et al., 1996*]. If an equivalent stretched Cartesian grid with global time stepping were used [*Raeder et al., 1995*], 25 times more computer time would be required, according to our best estimation.

3. Results

Here we describe the results of a run which had a piecewise constant IMF B_z, alternating between -5 nT and $+5$ nT with a period of one hour after an initial one-hour period of zero IMF. The solar wind velocity was kept at constant value of 420 km/s all the time. The solar wind proton number density was 7.3 cm^{-3} and the temperature was equal to 10^5 K. It is not possible to describe the output data exhaustively in this paper, and the reader should access our Web page `http://www.geo.fmi.fi/~pjanhune/gumics3/` for more colorful results and animations.

The IMF B_z input is displayed in **Figure 2**, middle curve. The figure also shows the total field-

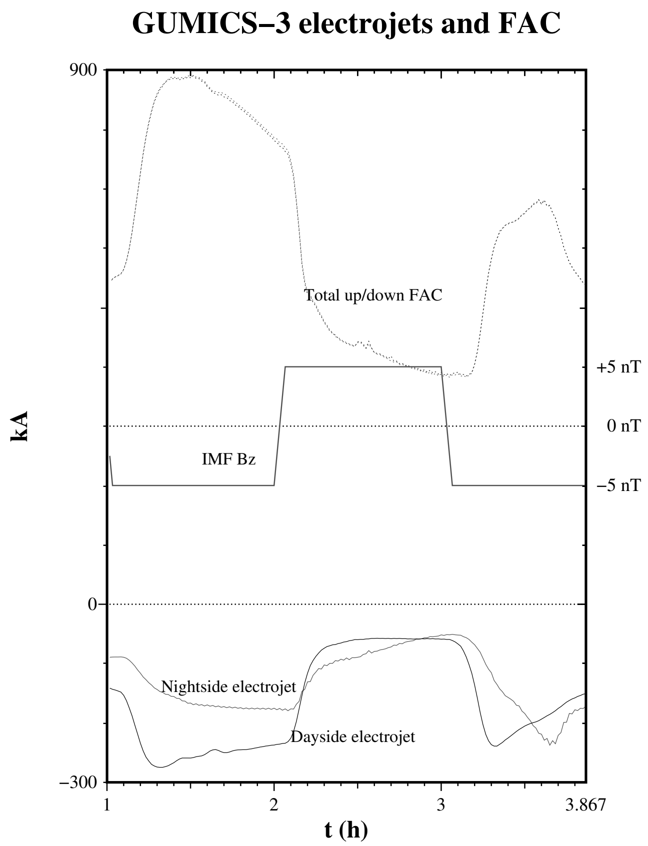

Figure 2: From up to down: Total upward/downward field-aligned currents (FAC) on northern hemisphere (maximum 890 kA); IMF (interplanetary magnetic field) B_z input; "dayside electrojet" and nightside electrojet magnitudes with minus sign. The upward/downward FAC curves almost overlap as they should (no charge should accumulate in the ionosphere). The "electrojet" quantities are obtained by integrating all current passing the constant magnetic longitude 0° (dayside) and 180° (nightside). On the nightside, this is a good estimate for the westward electrojet. On the dayside, the current is distributed over a wide area because the conductivity is more uniform due to solar UV contribution.

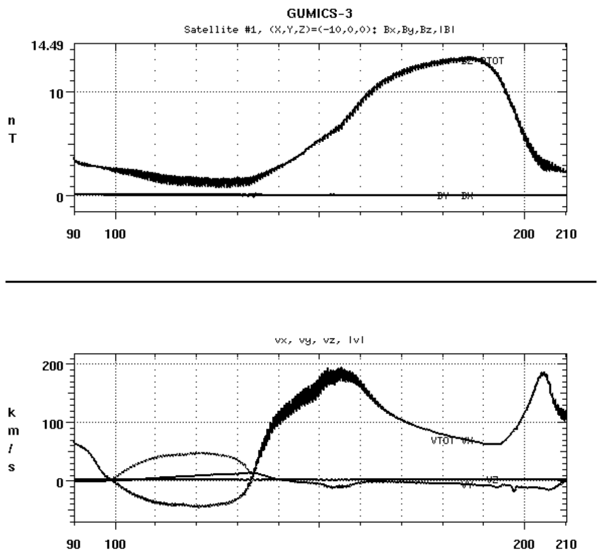

Figure 3: Simulated satellite data for a satellite at $(-10, 0, 0)$. Upper panel shows mainly B_z (B_x,B_y are very small). Lower panel shows the plasma velocity components; only v_x is significant. The time axis is in minutes from the start of the simulation (entry of solar wind).

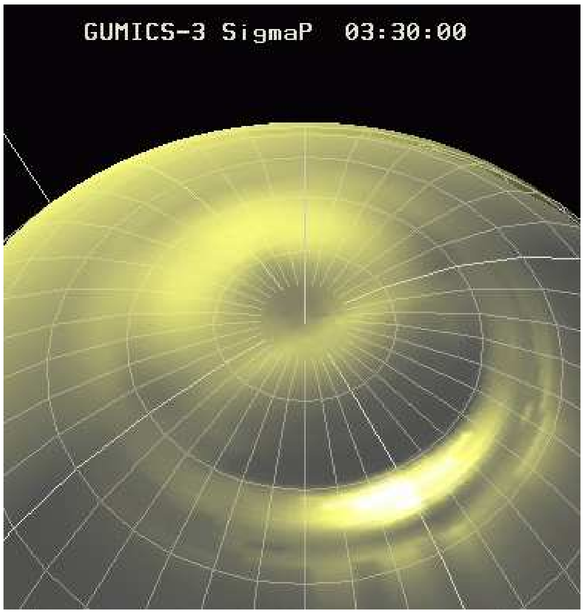

Figure 4: Example of simulated ionospheric height-integrated Pedersen conductivity distribution. An auroral activation and some small scale structures are seen on the nightside. On the dayside, the conductivity enhancment due to solar UV radiation is apparent. The peak Pedersen conductivity (on the nightside) is about 20 mho. The magnetic coordinate grid is also shown.

aligned current (FAC) entering and leaving the northern hemisphere ionosphere (uppermost two curves, which nearly overlap each other). The main contributor of these FACs is the Region-1 system. It is clear that the total FAC follows the IMF B_z variations faithfully, with about 10 min delay. When IMF is southward (-5 nT) the total FAC is about 700-800 kA. Other runs that we have performed but are not reporting here show that values exceeding 1 MA can be easily obtained by increasing the magnitude of IMF B_z. The lowest two curves in **Figure 2** are the total currents flowing in the dayside and nightside "electrojets". These are obtained by integrating the east/west current passing through a constant magnetic meridian, the $0°$ meridian in case of "dayside electrojet" and the $180°$ meridian in case of nightside electrojet. The sum of these two currents represents the total horizontal current flowing from the morningside to the eveningside. The nigthside electrojet thus defined flows mainly in the auroral oval, because the nightside ionospheric conductivity is low elsewhere. On contrast, the "dayside electrojet" is distributed over a wide area because the dayside conductivity is smooth. The total current flowing in both "electrojets" is smaller than the total FAC. This is because there is some closure horizontal current between the Region-1 and Region-2 systems, which does not have to flow from the morningside to the eveningside.

Figure 3 shows simulated satellite data from GUMICS-3. The satellite is at $(X, Y, Z) = (-10, 0, 0)$, i.e. in the near-Earth magnetotail at midnight meridian and in the equatorial plane. The upper panel shows B_z (the dipole contribution is included). At about $t = 150$ min, B_z starts to increase at the satellite position, a signature of dipolarization in the near-Earth region which is usually associated with substorm expansion phase. Before that B_z was getting smaller, which was a typical substorm growth phase signature. The lower panel shows fast (almost 200 km/s) earthward plasma flow associated with the dipolarization. The short variations in the curves are due to some MHD wave activity.

Figure 4 shows an example of the produced Pedersen conductivity pattern. The auroral luminosity is not directly related to the ionospheric conductivities, but the Pedersen conductivity gives a better impression of it than the Hall conductivity.

4. Discussion of the results

Let us discuss the promises and weaknesses of our model. The model can accept arbitrary solar wind input and a nonzero dipole tilt angle can be used, so the model is ready for application to real events. However, we can anticipate some degradation in the quality of the results for large dipole tilts because the tail current sheet will then move away from the $Z = 0$ plane and thus the densification of the grid is not exactly in the same location where the current sheet forms. This is not a serious problem, however, and can in principle be fixed by redesigning the grid point density function or by going to solution-adaptive grids [*Gombosi et al., 1996*]. Another problem is that the program might not converge for too violently varying solar wind input data. Using single satellite measurement of the solar wind directly (without averaging) might also be nonphysical in the sense that minute-scale variations in the data may in reality be local variations, which should not be interpreted as large-scale shock fronts. Thus the convergence problems in this case might not be problems with the code but problems with the physics. In any case, if convergence problems arise, one can try to cure them either by increasing the Δt CFL safety factor, which decreases Δt everywhere and thus increases the computing time but does not compromise the physics, or adding explicit diffusion, which does not increase the computing time but does alter the physics.

The model produces the overall geometry and current systems of the magnetosphere quite well. On the dayside, the bow shock, the magnetosheath, and the magnetopause can be clearly seen. The boundaries of the cusp are clear in plasma density and pressure (this was used as a measure of goodness of an MHD simulation by *Tanaka* [1994]). The Region-1 current system is always visible and its magnitude depends on the sign of IMF B_z. The closure path of Region-1 current system was studied already by *Janhunen et al.* [1996] using GUMICS-2, who found agreement with the results of *Tanaka* [1995]. The Region-2 current system is clearly weaker and it vanishes almost totally for northward IMF.

The simulation-produced Region-2 system may in fact be somewhat weaker than in reality. If this is the case, it may signify a too small plasma pressure in the very-near-Earth region. This in turn may arise because it takes a long time to get plasma to the very near-Earth region from the solar wind — longer than the duration of the simulation. Thus one should perhaps put some plasma in the near-Earth region explicitly in the beginning to get a stronger pressure gradient and thus a stronger ring current and stronger Region-2 current. With the accuracy of GUMICS-3 we are in any case able to study the closure path of Region-2 current also, but we shall not include this study in the current paper.

During northward IMF a current system develops close to the magnetic pole, which is similar to the so-called NBZ current system [*Ijima and Shibaji, 1987*]. After a period of southward IMF, substorm signatures (dipolarization, fast flows) are seen in the near-Earth magnetotail, together with enhanced Alfvén wave activity bouncing between the ionosphere and the magnetosphere. An auroral brightening is observed in the ionosphere at the same time. A substorm current wedge (SCW) can be identified in the ionosphere and we can trace it to the magnetosphere. However, the total current flowing in the wedge is only about 25 kA in the case simulated, which is insufficient of producing the negative magnetic "bay" in ground magnetograms, which is a typical substorm signature. Thus, although we can see numerous substorm signatures in our simulation, we still cannot say that we are simulating a real substorm because a well–developed SCW does not form. It may be that only by increasing the IMF variation magnitude we could increase the magnitude of the current wedge. Another possibility is that the simulated magnetotail is too short because of too poor grid resolution in the midtail region (around 20-50 R_E). This remains to be seen in future simulation runs. Increasig the resolution in regions where the dipole field is small introduces only a small increase in computing time. This is a virtue of the adaptive time stepping.

Maybe the most important weakness of the model, as far as harmful effects of energetic particles on satellites are concerned, is the lack of kinetic description of the plasma. The MHD equations do not properly describe situations where the velocity distributions are far from Maxwellian, neither do they describe pressure and temperature anisotropies. Thus we cannot predict energetic particle fluxes directly but must relate these to the MHD variables (pressure, density, temperature) by some indirect means. Related to the lack of kinetic description is the fact that we cannot compute the loss cone filling rate χ self-consistently but are forced to use an analytic model for it as was described above. This means that we cannot compute the electron precipitation and thus the ionospheric conductivities fully self-consistently. By changing our χ model we generally get different results. A related problem is also the electron temperature, which is also needed in Knight's [*Knight, 1973*] formula for precipitating electron flux. The MHD equations produce only a single plasma temperature (ion plus electron temperature), while experimental results indicate that the electron temperature is often significantly smaller than the ion temperature. Within MHD we have no self-consistent way of computing the temperature ratio.

5. Summary

A global ionosphere-magnetosphere coupling simulation model has been presented. By using the Roe type linearized Riemann solver together with an unstructured spatial grid, locally varying adaptive time stepping, and separated, analytic treatment of the dipole magnetic field, we have obtained a resolution in the near-Earth region that has not been achieved before. The only essential input for the model is the solar wind time series. As outputs we get the MHD variables in the magnetoshpere and the conductivities, currents and electric potential in the ionosphere as a function of time. A run with piecewise constant interplanetary magnetic field (IMF) was presented. It produced many substorm related features both in the ionosphere and in the near-Earth magnetotail after about 45 minutes of southward IMF. The remaining problem areas are mainly in the very-near-Earth region, where non-MHD processes may be important and where the inner boundary conditions have an effect on the solution.

Our near future plans include performing runs with real solar wind data. Many figures and animations related to this work can be found using WWW at `http://www.geo.fmi.fi/~pjanhune/gumics3/`.

References

Fedder, J. A., Lyon, J. G., Slinker, S. P., Mobarry, C. M., Topological structure of the magnetotail as a function of interplanetary magnetic field direction, J. Geophys. Res., 100, 3613–3621, 1995.

Fridman, M. and Lemaire, J., Relationship between auroral electrons (sic) fluxes and field aligned electric potential difference, J. Geophys. Res., 85, 664–670 1980.

Gombosi, T.I., DeZeeuw, D.L., Häberli, R.M. and Powell, K.G., Three-dimensional multiscale MHD model of cometary plasma environments, J. Geophys. Res., 101, 15233–15253, 1996.

Ijima, T. and Shibaji, T., Global characteristics of northward IMF-associated (NBZ) field-aligned currents, J. Geophys. Res., 92, 2408–2424, 1987.

Janhunen, P. and Huuskonen, A., A numerical ionosphere-magnetosphere coupling model with variable conductivities, J. Geophys. Res., 90, 9519–9530, 1993.

Janhunen, P., Pulkkinen, T.I., and Kauristie, K., Auroral fading in ionosphere-magnetosphere coupling model: Implications for possible mechanisms, Geophys. Res. Lett., 22, 2049–2052, 1995.

Janhunen, P., Koskinen, H.E.J., Pulkkinen, T.I., A new global ionosphere-magnetosphere coupling simulation utilizing locally varying time step, in Proceedings of Third International Conference on Substorms (ICS3), Versailles, France, May 12-17, ESA SP 1996.

Janhunen, P., Tela the Tensor Language: A scientific computing environment, `http://www.geo.fmi.fi/prog/tela.html`, 1994-1996.

Knight, S., Parallel electric fields, Planet. Space Sci., 21, 741–750, 1973.

LeVeque, R.J., Numerical methods for conservation laws, Birkhäuser, 1992.

Lundstedt, H. and Wintoft, P., Prediction of geomagnetic storms from solar wind data with the use of a neural network, Ann. Geophys., 12, 19–24, 1994.

Ma, Z.W., Hawkins, J.G., Lee, L.C., A simulation study of impulsive penetration of solar wind irregularities into the magnetosphere at the dayside magnetopause, J. Geophys. Res., 96, 15751–15765, 1991.

Ogino, T., A three-dimensional MHD simulation of the interaction of the solar wind with the earth's magnetosphere - The generation of field-aligned currents, J. Geophys. Res., 91, 6791–6806, 1986.

Press, W.H., S.A. Teukolsky, W.T. Vetterling, and B.P. Flannery, Numerical Recipes in C: The art of scientific computing, 2nd edition, Cambridge, 1992.

Raeder, J., Walker, R. J., Ashour-Abdalla, M., The structure of the distant geomagnetic tail during long periods of northward IMF, Geophys. Res. Lett., 22, 349–352, 1995.

Tanaka, T., Finite volume TVD scheme on an unstructured grid system for three-dimensional MHD simulation of inhomogeneous systems including strong background potential fields, J. Comp. Phys., 111,, 381–389, 1994.

Tanaka, T., Generation mechanisms for magnetosphere-ionosphere current systems deduced from a three-dimensional MHD simulation of the solar wind-magnetosphere-ionosphere coupling processes, J. Geophys. Res., 100, 12057–12074, 1995.

Vassiliadis, D., Klimas, A.J., Baker, D.N., Roberts, D.A., A description of the solar wind-magnetosphere coupling based on nonlinear filters, J. Geophys. Res., 100, 3495–3512, 1995.

Watanabe, K. and Sato, T., Global simulation of the solar wind-magnetosphere interaction - The importance of its numerical validity, J. Geophys. Res., 95, 75–88, 1990.